Reaction Kinetics of One-Pot Xylan Conversion to Xylitol via Precious Metal Catalyst

Gerd Hilpmann, Pascal Kurzhals, Tom Reuter and Mick Miro Ayubi*

Chair of Chemical Engineering and Process Plants, Institute of Process Engineering and Environmental Technology, Technische Universität Dresden, Dresden, Germany

The hydrolytic hydrogenation of xylan to xylitol by a one-pot process was studied in detail in a batch reactor. The reaction was catalyzed by a combination of diluted sulfuric acid and precious metal Ru on carbon powder. Process parameters were varied between 120–150°C, while maintaining constant hydrogen pressure at 20 bar and an acid concentration equivalent to pH 2. The xylan solution consisted of 1 wt% beechwood powder (Carl Roth, >90%) in deionized water. Sulfuric acid was added to the solution until pH two was reached, then the 0.3 wt% catalyst powder (5% Ru on Act. C) was added and the solution was put into the batch reactor. The first approach of kinetic modeling began with conventional first-order kinetics and compared this to a more complex model based on Langmuir–Hinshelwood kinetics. The xylan and xylitol data reached a good fit. However, the modeling results also showed that the rate-limiting step of xylose-formation was still not represented in a satisfactory manner. Therefore, the model was adapted and developed further. The advanced model finally showed a good fit with the intermediate product xylose and the target product xylitol. The overall modeling methods and results are presented and discussed.

Keywords: one-pot reaction, xylan, xylitol, reaction kinetics, hydrolytic hydrogenation, kinetic modelling

INTRODUCTION

Since the start of the ongoing debate on global warming, the research in many scientific fields has focused more and more on environmentally friendly and sustainable approaches. In the chemical industry, this trend led to the development of biorefinery concepts with the aim of producing fuels and fine chemicals from renewable resources. This "green chemistry" could use waste plant material from the agricultural and wood industry as feedstock. Ideally, this biorefinery feedstock should be of almost completely non-food biomass origin. Recent research was mostly focused on the processing of cellulose, as it is the most abundant part in many plant species (Kamm and Kamm, 2004; Chheda et al., 2007; Anwar et al., 2014; Fagerstedt et al., 2014; Wirsching, 2014). However, it is conceivable that there will be an increased need for experimental data on processing hemicelluloses with the advancing development of biorefinery processes. The conversion of hemicelluloses is usually conducted with the aim to convert them to monosaccharides. These monosaccharides are valuable chemicals for food, cosmetic and pharmaceutical industries. They might also be further converted into polyols, also known as sugar alcohols. A very prominent sugar alcohol is xylitol (E967) due to its broad market application as a sweetening supplement in diabetic-friendly food and as an anti-cariogenic in toothpastes and chewing gums (Delgado Arcaño et al., 2020; Liu et al., 2019). Xylitol can be derived from the monosaccharide xylose, the main structural component of xylan.

This very common hemicellulose is most abundant in birchwood, beechwood and corn residues (Teleman et al., 2002; Westbye et al., 2008; Bigand et al., 2011; Sedlmeyer, 2011; Ji et al., 2012), and therefore fits the ecological requirement as non-food biomass very well.

The process route from xylan to xylitol requires firstly (after biomass pretreatment) the cleavage of glycosidic bonds between xylose monomer units and its counterparts, which could be other xylose molecules or different chemical constituents of xylan. Depending on its plant origin, these can be 4-O-methyl-glucuronic acid, acetyl groups (Gellerstedt and Henriksson, 2009; Mäki-Arvela et al., 2011). Subsequently, the second process step realizes the conversion of xylose to xylitol. This process chain requires catalytic reactions to take place for a successful conversion, which typically applies acids, bases or enzymes for the cleavage to xylose and precious supported metals or yeasts for the refinement to xylitol. Both individual process steps and their most efficient catalysts have been studied in great detail (Sun and Cheng, 2002; Mäki-Arvela et al., 2011; Testova et al., 2011; Salmi et al., 2014a; Renard et al., 2014; Saleh et al., 2014; Vandenbossche et al., 2014; Hernandez-Mejia et al., 2016). However, recent advancements in process intensification technologies led to the development or rebirth of the concept known as one-pot processing, wherein two entirely different, typically apart catalysts are applied within the same reactor ("one-pot") for the benefit of cost, time and resource reduction. In the context of chemical biomass conversion, this concept was discussed as early as 1960 for the hydrolytic hydrogenation of wood biomass, but unfortunately was dismissed too early (Vasyunina et al., 1960; Sharkov, 1963). The researchers investigated the combination of acidic hydrolysis (H_3PO_4, HCl, H_2SO_4) with metal catalyzed hydrogenation (Ru on C powder), thus called "hydrolytic hydrogenation", and proposed that the increased temperature and pressure helps both catalytic reactions and enables the one-pot process of cellulose conversion to glucose with integrated subsequent refinement towards sorbitol, sparing one additional process step.

Nowadays, this idea seems to be a possible answer to the question of whether biorefineries could compete commercially with traditional fossil-based refinery technologies. Therefore, researchers recently started to investigate many different combinations of catalysts, both of chemical of biotechnological origin, with the aim to develop novel hybrid processes based on the one-pot process concept.

Ribeiro et al. conducted experiments on the hydrolytic hydrogenation of xylan obtained from corn cobs using a Ru/C nanotube catalyst with a metal load of 0.4 wt% by weight, without the use of acids or a further catalyst for hydrolysis. The reaction was carried out under 50 bar hydrogen pressure and at a temperature of 205°C for up to 5 h. The maximum xylan yield of 46.3 wt% was achieved after 45 min. In further experiments the influence on the formation of xylitol in the presence of cellulose in the reaction solution was to be investigated. The xylitol yield increased to 60 wt% in less than 1 h due to the presence of cellulose. In addition, a sorbitol yield of 80 wt% in 2 h reaction time was recorded (Ribeiro et al., 2016).

Based on the results mentioned above, Ribeiro et al. performed further experiments on the simultaneous conversion of cellulose and xylan. The experiments were performed at 50 bar hydrogen pressure for up to 8 h using the same Ru/C nanotube catalyst as in the previous experiments. The evaluation of the experiments showed that the yield of xylitol and sorbitol is maximized by conversion using a two-step temperature program. In the first step, the reaction was carried out at 170°C for 2 h, after which the temperature was increased to 205°C for a further 4 h. This temperature control of the reactor resulted in a yield of xylitol and sorbitol of 77 and 75 wt% respectively. Xylan or cellulose did not achieve the same or higher yields in selective, i.e. non-simultaneous hydrolytic hydrogenation, neither with the identical two-step temperature program nor with the corresponding individual constant temperatures, varying between 170 and 205°C (Ribeiro et al., 2017).

Dietrich et al. used various heteropolyacids and organic acids in combination with ruthenium, added to carbon (5 wt%), for their investigations. The experiments were performed at 140°C and 20 bar hydrogen pressure, using xylan obtained from beech wood. The use of lactic acid or tungstophosphoric acid in combination with hydrogen and the Ru/C catalyst led to a xylitol yield of about 70 wt% within a hydrogenation time of 3 h. The working group also used isopropanol as an alternative hydrogen donor to realize a transfer hydrogenation. The combination of tungstophosphoric acid and isopropanol in combination with the Ru/C catalyst resulted in an increase of the xylitol yield by 12–82 wt%. In contrast, lactic acid in this combination produced only about 20 wt% xylitol yield. This is probably due to a parallel esterification reaction (Dietrich et al., 2017).

Lie et al. carried out one-pot experiments to convert real biomass (corn stalk) using a Ru/C catalyst into liquid alkylcyclohexanes and sugar alcohols. The experiments were performed at 473 k (sugar alcohols), 573 K (liquid alkylcyclohexanes) and 20 bar hydrogen pressure. The xylitol yield was 12.2 wt%, the sorbitol yield 24.5 wt% and the C2–C4 polyols yield was 16.0 wt%. The yield of liquid alkylcyclohexanes based on the lignin contained in the substrate was 97.2 wt%. The authors underline the important role of the synergetic effect between Ru and RuO2 on the Ru/C catalyst for the catalysis (Li et al., 2018).

The authors Barbaro, Liguori and Moreno-Marrodan carried out one-pot experiments with a bifunctional catalyst consisting of a Brønsted solid acid (Ru@Dowex-H) as carrier for ruthenium for the synthesis of anhydrous sugar alcohols. The experiments were performed at a temperature of 393 k, a hydrogen pressure of 30 bar and a reaction time of 7 h. Yields of 1,4-anhydroxylitol of 94% were achieved (Barbaro et al., 2016).

One-pot conversion of lignocellulosic biomass into alkylcyclohexane and polyols using Ru/C and H2 in water was reported by Wang et al. (Li et al., 2018).

The one-pot conversion of real biomass (bagasse) at a temperature of 463 K, a pressure of 5 MPa and a reaction time of 16 h in a batch reactor was published by the authors Yamaguchi et al. The experiments achieved a sugar alcohol yield of 50.6%. This process is one step of a concept for the

conversion of lignocellulose into valuable chemicals (Yamaguchi et al., 2019).

Our own research started to push open the window for the combined application of chemical and biological/biotechnological catalysts for biorefinery applications, which were historically utilized separately (Hilpmann et al., 2019; Ayubi et al., 2020).

However, these explorative studies are yet to formalize their findings into models, based on which biorefineries may be designed and further optimized. Therefore, our research focused on the application of well-established catalyst for the hydrolytic hydrogenation of xylan to xylitol, specifically, hydrochloric acid and ruthenium (on carbon powder). Both individual process steps, hydrolysis and hydrogenation, and their respective catalytic reactions have a broad knowledge base and first kinetic models were readily published (González et al., 1986; Jacobsen and Wyman, 2000; Lu and Mosier, 2008; Kusema et al., 2010; Liu et al., 2012; Sifontes Herrera et al., 2012; Salmi et al., 2014b; Zhao et al., 2014; Zhu et al., 2014; Nakasu et al., 2017; Li et al., 2019). We would like to contribute an approach into modeling the reaction kinetics of the one-pot process "hydrolytic hydrogenation" of the exemplary biomass resource xylan, to develop a base for future kinetic models and therefore hopefully enabling more efficient biorefinery processes.

MATERIAL AND METHODS

Chemicals and Catalysts

The water for the experiments was purified by laboratory equipment via two steps. First, it was supplied from a desalination system and then treated in a deionization apparatus (TKA MicroPure). The educt xylan was commercially retrieved from the company Carl Roth GmbH, with a purity of ≥90%, originated from beechwood.

The precious metal catalyst powder consisted of 5% ruthenium on activated carbon, commercially retrieved as wetted powder with 50–70% H_2O from the company abcr GmbH ("Evonik H 198 P/W 5% Ru"). To ensure comparability to other relevant research activities in the field, our applied catalyst was selected with similar general characteristics as the Ru/C catalyst characterized in great detail by Sifontes et al. (Sifontes Herrera et al., 2011). Own catalyst characterization could not be realized due to lack of suitable analysis systems. The catalyst needed to be activated before each individual experimental run at 140°C with 10 bar gaseous H_2 for at least 4 h, as the rapid catalyst deactivation had been observed earlier (Hilpmann, 2017).

Experimental Setup

The whole setup was located inside a common laboratory fume hood. The main technical systems were two independent heating/cooling systems, a reactor control system, and the reactor system itself. A heating system with a thermal oil bath was connected to the reactor's jacket via two isolated flexible tubes. It was also used for measuring the temperature inside the reactor with a pt100 temperature sensor and for manually controlling the reactor temperature. The other system was used as supply of cooling water for the reactor's stirring unit.

The reactor control system was provided by the same company as the stainless steel reactor itself (model: 5100, company: Parr Instrument). It was used to measure the pressure in the reactor (bar) and to control the revolution speed of the stirrer (rpm). Next to the reactor was installed the armature for the gas inlet pressure. It was connected to gas inlet valves for hydrogen and nitrogen via Swagelok® tubes and T-pieces. This armature was used to pre-set the gas pressure in the reactor to the designated value and to control the gas flow into the reactor.

Reactor

The reactor head was equipped with an armature with a connector for a pressure measuring sensor and two openings, leading process gas into the reactor and vice versa taking liquid samples from the reaction mass through a separate valve via the sample tube, equipped with an exchangeable filter fitting. The stirrer was equipped with a gas entrainment impeller which provided an effective suspension of tiny gas bubbles (here: hydrogen) into the aqueous reaction solution at a minimum stirrer speed of 700 rpm. The discontinuous reactor consisted of the reactor head (fixed) and the reactor vessel which were sealed by an o-ring and closed by a split-ring-sealing. The stainless steel reactor vessel can be can be operated at harsh reaction conditions (max. 40 bar, 250°C).

Sampling Procedure

Samples with a volume of 5 ml have been taken through the reactor tube after rinsing it with the same volume of pre-sample liquid. Due to the acidic hydrolysis, the samples needed immediate further treatment to stop the reaction. Therefore, the sample liquid was cooled down by placing the sample container in an icy water bath. After that, the sample liquid, still at acidic pH value, was neutralized with a 0.1 M NaOH/water solution. The mass of neutralization agent added to each sample was measured with a labor balance to recalculate concentrations within the sample liquid later. Smaller amounts of liquid volume were taken from the original samples for further analysis preparation. Afterwards, the original samples were put into a refrigerator to deep freeze (about −18°C) them for long-term storage.

Experimental Procedure

At the beginning of every experimental run, the heating system was preheated to provide an initial reactor temperature of up to ca. 50°C, thereby decreasing the system's hysteresis during the heating ramp to the desired final temperature. This was deemed to be a good value, because at this temperature the reactor could still be handled safely. The water for the reaction solution was weighed to 280 g before every experiment. Upon gathering the same correct amount of water into a 300 ml glass beaker each time, 3 g of xylan have been added, followed by stirring with a magnetic stirrer on a common stirring plate to accelerate the otherwise lengthy dissolution process of xylan in water. With a 100 μl Eppendorf-pipette, droplets of concentrated sulfuric acid
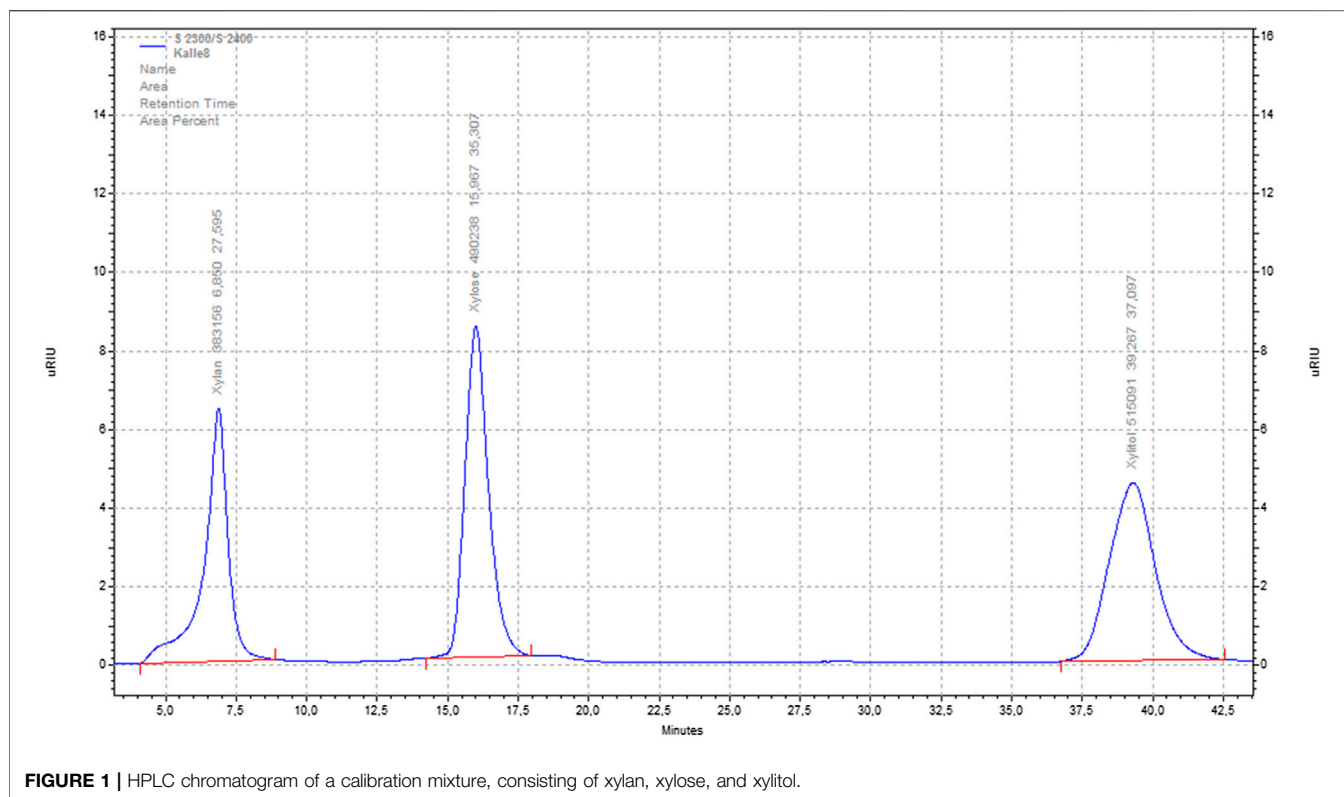
FIGURE 1 | HPLC chromatogram of a calibration mixture, consisting of xylan, xylose, and xylitol.

were added (95–97%) until the desired pH value of two was reached (measured with pH-meter Mettler Toledo LnLap Expert Pro pH and Mettler Toledo SevenEasy). Any remaining solid xylan blocks were successfully dissolved at last after adding the acid. Finally, 0.9 g of Ru/C catalyst were weighed and added to the prepared solution. Upon short mixing with the magnetic stirrer, the solution was put into the reactor which was then tightly closed.

After the last sample had been taken, the heating was switched off and the hydrogen pressure was released through a valve at the reactor head which was connected to the exhaust of the fume hood. Then, the reactor was rinsed three times with nitrogen at 6 bar. The pressure was released completely, and the reactor was left to cool down.

Chemical Analysis via HPLC
Sample Preparation
Before any sample liquid injection into the HPLC, all samples were filtrated with 0.2–0.45 μm syringe filters to prevent possible damage to the separation column by micro-particles or plugging due to agglomerated molecules, eg partially hydrolyzed xylan block molecules or larger xylo-oligomers. Moreover, the neutralization agent $CaCO_3$ could be easily separated during the sample filtration.

HPLC Equipment and Method
The samples of our experiments were analyzed in a "Smartline"® HPLC of the company Knauer GmbH. For analysis of hemicelluloses and their conversion products (see **Figure 1**), a
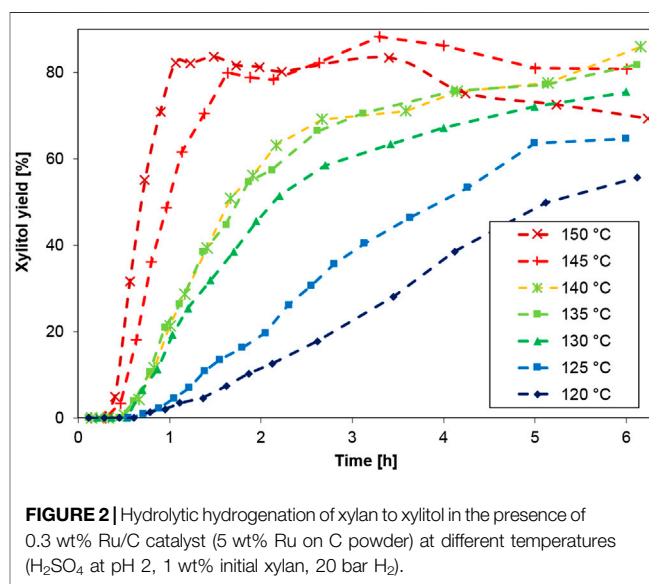

FIGURE 2 | Hydrolytic hydrogenation of xylan to xylitol in the presence of 0.3 wt% Ru/C catalyst (5 wt% Ru on C powder) at different temperatures (H_2SO_4 at pH 2, 1 wt% initial xylan, 20 bar H_2).

typical 'sugar column' was installed to the RI detector (Smartline® RI 2300). Thus, the column line consisted of a pre-column (Eurokat-Pb 30 × 8mm, 10 μm) and a separation column (Knauer GmbH, model Eurokat-Pb 300 × 8mm, 10 μm); both were heated inside a column oven (Jetstream 2).

The analytical method was as follows: 20 μl of sample was injected; the eluent was deionized and ultrasonic-assisted-degassed water with a flow rate of 0.6 ml/min. The column
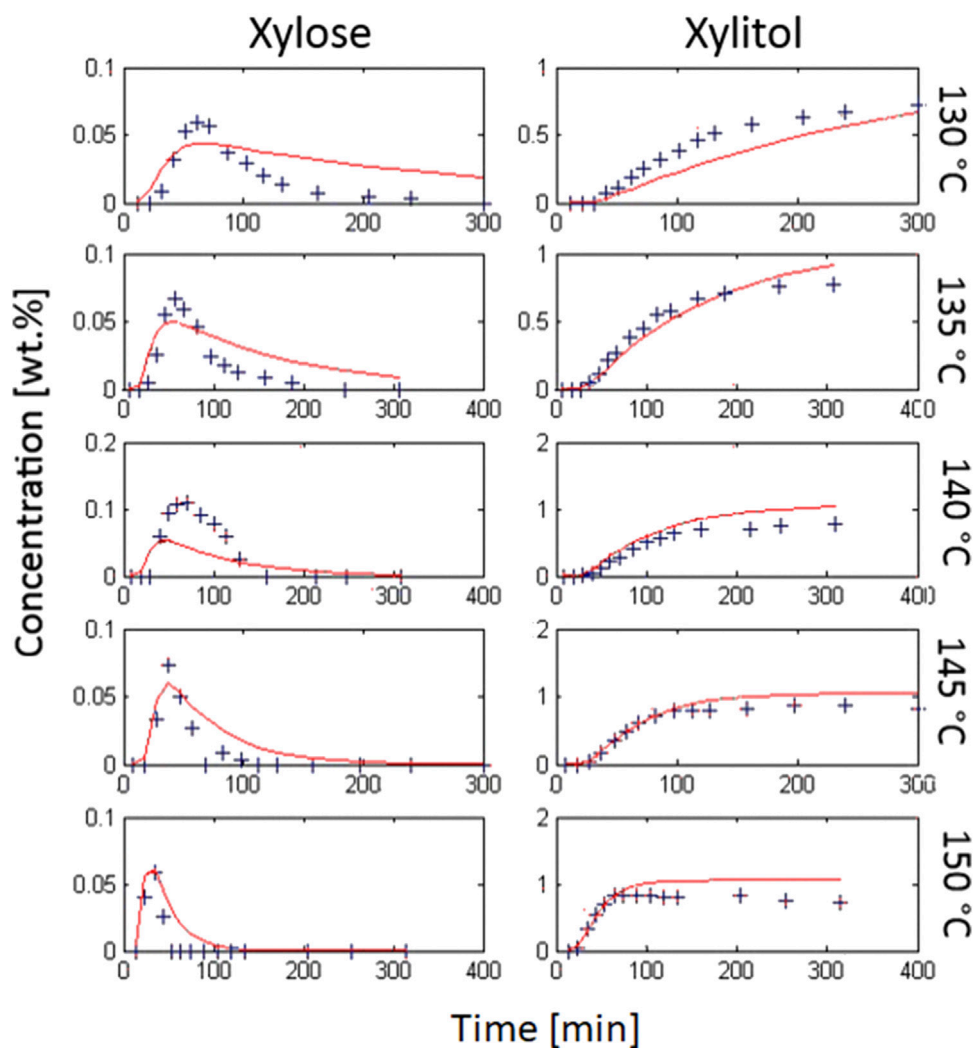
FIGURE 3 | Simple second order kinetic model; calculation (red) vs. experimental data (blue cross) from hydrolytic hydrogenation; 1 wt% initial xylan, 0.3 wt% Ru/C catalyst (3.5 wt% Ru on C powder, H_2SO_4 at pH 2, 20 bar H_2).

oven was set to a temperature of 75°C. A typical sample run took about 60 min. In between different samples, clear water was injected as intermediate clean-and rinse-run at the same conditions for at least 20 min.

EXPERIMENTAL RESULTS

The most representative experimental data is shown for the target product xylitol in **Figure 2**. The graph clearly elucidates the temperature dependency of xylitol production from xylan, via the intermediate xylose, in the range of 120–150°C. The respective concentration curves of xylan and xylose are shown later in context of evaluating the different modeling approaches of reaction kinetics to avoid duplet graphical representation.
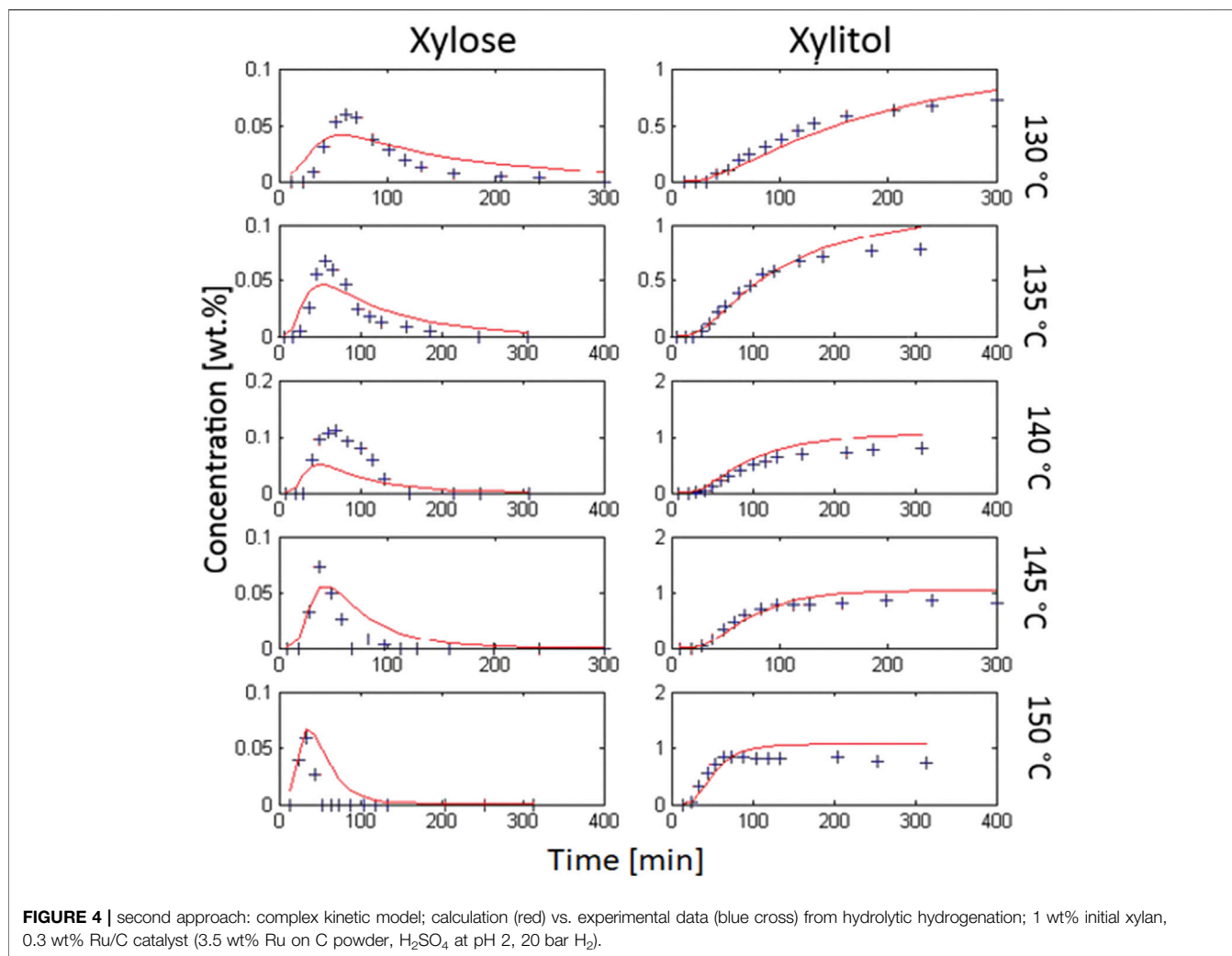
Upon studying the xylitol yield curves, the acceleration of the reaction rate with each temperature increment of +5 K becomes obvious. Therefore, the modeling approach for the reaction

kinetics seems to call for the application of Arrhenius kinetics, considering the catalytic hydrogenation via Ruthenium on Carbon powder. The experimental data also points towards an optimal process window for the hydrolytic hydrogenation of xylan to xylitol. The turnover-frequency (TOF) was calculated according to the widely accepted formula

$$TOF = \frac{r_{xylitol}}{c_{catalyst}} = \frac{\Delta c_{xylitol}}{\Delta t^* c_{catalyst}}$$

wherein the catalyst concentration is applied as catalyst loading in the reaction solution (here: 1 wt%) and the xylitol formation rate is calculated via the HPLC-measured concentrations; the rate was calculated within the linear steep range of the individual curves (see **Table 1**).

To reach the highest xylitol yields above 80% after 6 h, the reaction should take place at 135°C or more. However, while further temperature increase can shorten the process duration to under 2 h, a too-harsh temperature at 150°C leads to rapid

FIGURE 4 | second approach: complex kinetic model; calculation (red) vs. experimental data (blue cross) from hydrolytic hydrogenation; 1 wt% initial xylan, 0.3 wt% Ru/C catalyst (3.5 wt% Ru on C powder, H_2SO_4 at pH 2, 20 bar H_2).

product degradation. The formation of by-products had been investigated earlier via GC-MS and revealed that additionally formed compounds were arabinose, erythrose, arabinofuranose, glucitol, galactofuranosides, xylulose, ribonic acid, and glucopyranose (Hilpmann, 2017). The data set from the experiment at 140°C or 135°C, in contrast, seems slightly off the trend of the rest of the experiments for (until now) unknown reasons, yet still provides us with further data points, which is why we decided to include it into the data base for the kinetic modeling. It should also be noted that the initial observable delay of the reaction start (ca. 20–30 min) can be mostly attributed to heating hysteresis of the reactor system. Yet, we decided to include the experimental data into the modeling data to have a robust set of 'zero'-samples for each experiment.
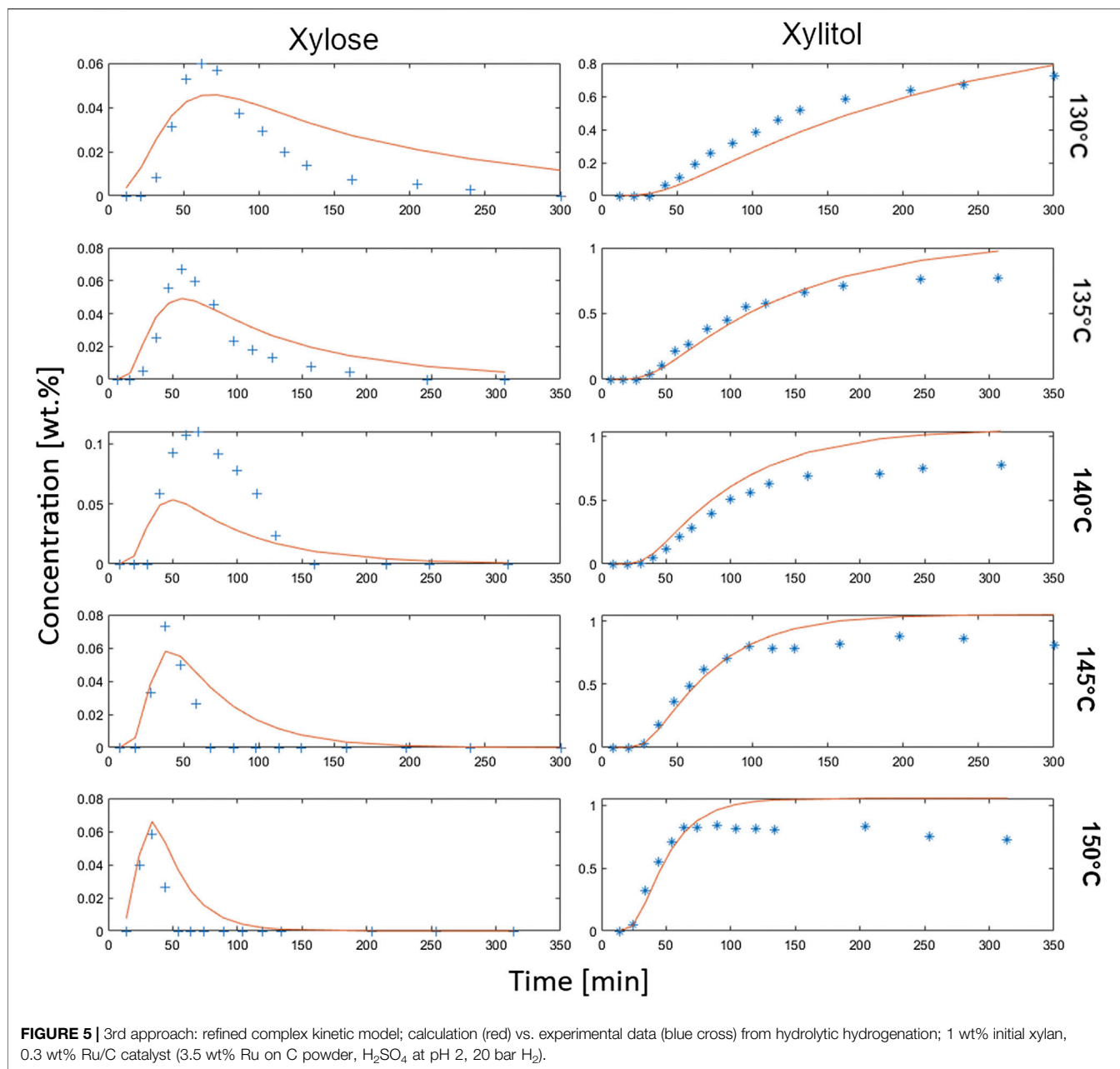
MODELING OF REACTION KINETICS

Both acid hydrolysis and metal catalyzed hydrogenation have been modeled before to quite some extent as we discussed in the introduction. In contrast, modeling reaction kinetics of the

complex one-pot process of hydrolytic hydrogenation is still a largely unexplored field in the context of hemicellulose conversion. However, first steps into that rather unknown valley were undertaken with the aid of model approaches from the literature. The whole chapter is therefore divided into three subchapters, wherein we present and discuss first a model based on generalized second order reaction kinetics. This approach is followed by a more complex model, including relevant reaction steps of the main reaction pathway(s). Finally, we describe an optimized model which combines the complex model with recent literature findings and own parameter adaptations.

First Approach: Generalized Second-Order Model

Our first approach towards modeling the reaction kinetics of the hydrolytic hydrogenation of xylan to xylitol focus on established approaches for hemicellulose hydrolysis and sugar hydrogenation. Thus, a strong focus lay on the incorporation of the two most influential process parameters pH value and temperature, via concentration of effectively available protons

FIGURE 5 | 3rd approach: refined complex kinetic model; calculation (red) vs. experimental data (blue cross) from hydrolytic hydrogenation; 1 wt% initial xylan, 0.3 wt% Ru/C catalyst (3.5 wt% Ru on C powder, H_2SO_4 at pH 2, 20 bar H_2).

(here via C_{H2O}) and Arrhenius law kinetics. To apply the latter, we needed to narrow down the experimental data on the temperature range of 130–150°C. Otherwise the model would rely its calculations on data from experiments with non-complete conversion (xylitol yield far below 80%) and deliver much higher deviations from the actual experimental results. The generalized approach for the reaction kinetics focused on three of the main chemical reactions:

(1) Hydrolysis of xylan to xylo-oligomers (polysaccharides with $9 > n_{xylose} > 1$),
(2) Hydrolysis of xylo-oligomers to xylose monomers,
(3) Hydrogenation of Xylose to Xylitol.

It was reported previously that xylan is converted to xylo-oligomers very fast, compared to the cleavage of oligomers to monomers (Hilpmann et al., 2016). Moreover, the concentrations of the different oligomer factions could not be measured quantitatively in a reproducible fashion, which seems to remain a technical challenge until now, as relevant literature also retorts to hemicellulose and/or sugar measurement. Thus, the modeling approach focused on the rate-limiting step of xylose formation (from oligomers) and its subsequent conversion to xylitol.

To facilitate the model calculations, the concentration of the overall amount of intermediate xylo-oligomers was calculated by subtraction of the measured products from the initial xylan

amount, because by-products or deformation of xylose or xylitol played a negligible role at the applied process conditions:

$$C_{oligo} = C_{xylan,0} - C_{xylose} - C_{xylitol}$$

With respect to the main reaction mechanism of hydrolysis, the cleavage by protonation, it is a viable approach to assume that each successful cleavage reaction requires one dissociated water molecule (C_{H2O}). Thus, the rate equations for xylose and xylitol are denoted as follows:

$$\frac{dC_{xylose}}{dt} = k_1 \, C_{H_2O} \, C_{oligo} - k_2 \, C_{H_2} \, C_{xylose}$$

$$\frac{dC_{xylitol}}{dt} = k_2 \, C_{H_2} \, C_{xylose}$$

The results of the calculations are plotted together with the experimental data **Figure 3**. Please note that the xylose concentrations are typically one order of magnitude smaller than the xylitol concentrations due to the small time window between xylose-cleavage from xylan and its subsequent hydrogenation to xylitol.

The graph indicates that the model fits well for most xylitol data, except the experimental results from hydrogenation at 130°C. However, the curve fit of the xylose data was satisfactory only for experiments at 145 and 150°C. The mean error R was 4.03%. The constants from Arrhenius law are given here, while the other parameters k_i are given in an overview table at the end of the chapter.

$$\text{Xylose: } k_\infty = 1,0715 \cdot 10^{20} \quad E_A = 1,7320 \cdot 10^5$$

$$\text{Xylitol: } k_\infty = 5,4315 \cdot 10^{21} \quad E_A = 1,1889 \cdot 10^5$$

With our next modeling approach, we wanted to improve the model fit for both xylitol and xylose.

Second Approach: Complex Model

The first approach followed a rather holistic and generalized model with a very superficial look on the two relevant catalysis mechanisms, namely acid-base catalysis and precious metal surface catalysis. With the second approach, we therefore had put strong effort into considering all relevant reaction steps during the most prevalent catalytic reactions taking place during the (dual catalyzed) one-pot conversion of xylan to xylitol. The following complex model basically combines hydrolysis kinetics (via acid-base catalysis) with Langmuir-Hinshelwood kinetics for the Ruthenium powder catalyst. The model includes several reaction steps of hydrolysis, adsorption, hydrogenation, and desorption.

We present the stepwise reaction by the most relevant and rate-limiting steps. For the homogeneously acid catalyzed hydrolysis the three main steps have been defined as follows:
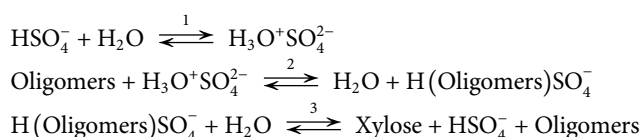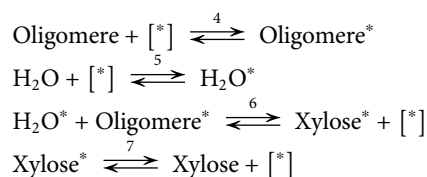
$$HSO_4^- + H_2O \underset{}{\overset{1}{\rightleftarrows}} H_3O^+SO_4^{2-}$$

$$\text{Oligomers} + H_3O^+SO_4^{2-} \underset{}{\overset{2}{\rightleftarrows}} H_2O + H\,(\text{Oligomers})SO_4^-$$

$$H\,(\text{Oligomers})SO_4^- + H_2O \underset{}{\overset{3}{\rightleftarrows}} \text{Xylose} + HSO_4^- + \text{Oligomers}$$

TABLE 1 | TOF values for the different experiments.

| T (°C)	120	125	130	135	140	145	150
TOF (1/h)	0.12	0.11	0.26	0.38	0.47	0.87	0.95

TABLE 2 | Test of different variations of the model modifications.

Model variation	Mean error R {%}
$k_5 = 0$, 85% mean xylitol yield	4,3051
$k_5 = 0$, $k_6 = 1$, 85% mean xylitol yield	5,1928
$k_3 = 1$, $k_5 = 0$, $k_9 = 0$ 85% mean xylitol yield	5,8462
$k_5 = 0$, $k_6 = 1$, 85% mean xylitol yield, parallel hydrolysis	4,0679
$k_5 = 0$, 85% mean xylitol/xylose yield	4,6116
$k_5 = 0$, $k_6 = 1$, 85% mean xylitol/xylose yield	3,9629

With respect to the very slow oligomer hydrolysis, we also considered the heterogeneously co-catalyzed hydrolysis in presence of Ruthenium. The designated partial reaction steps were formulated based on Langmuir–Hinshelwood reaction kinetics. Thus, the formula [∗] denotes any free active catalytic site on the catalyst surface. A specific molecular species with ∗ describes an adsorbed molecule on this active catalyst site.

$$\text{Oligomere} + [^*] \underset{}{\overset{4}{\rightleftarrows}} \text{Oligomere}^*$$

$$H_2O + [^*] \underset{}{\overset{5}{\rightleftarrows}} H_2O^*$$

$$H_2O^* + \text{Oligomere}^* \underset{}{\overset{6}{\rightleftarrows}} \text{Xylose}^* + [^*]$$

$$\text{Xylose}^* \underset{}{\overset{7}{\rightleftarrows}} \text{Xylose} + [^*]$$

The hydrogenation of xylose to xylitol was then denoted in a similar manner:

$$H_2 + 2[^*] \underset{}{\overset{8}{\rightleftarrows}} 2H^*$$

$$2H^* + \text{Xylose}^* \underset{}{\overset{9}{\rightleftarrows}} \text{Xylitol}^* + 2[^*]$$
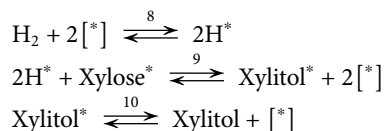
$$\text{Xylitol}^* \underset{}{\overset{10}{\rightleftarrows}} \text{Xylitol} + [^*]$$

The carbon balance with all the newly defined reaction rate constants can be thus defined as:

$$\frac{dC_{xylose}}{dt} = k_{hydro} \, C_{oligo} \, 10^{-2 \, pH} + \frac{dC_{xylose,*}}{dt \, K_7 \, C_*}$$

$$\frac{dC_{xylitol}}{dt} = \frac{dC_{xylitol,*}}{dt} \frac{1}{K_{10} \, C_*}$$

$$= \frac{C_*^2}{K_{10}} \left(K_8 \, K_{9+} \, C_{H_2} \frac{C_{xylose}}{K_7} - K_{9-} \, K_{10} \, C_{xylitol} \right)$$

The modeling results (see **Figure 4**) did not obviously improve or change significantly, compared to the first approach. The model delivered the following values for the rate constant and activation energies for the xylose and xylitol formation, respectively:

$$\text{Xylose: } k_\infty = 1,4277 \cdot 10^{19} \quad E_A = 8,0858 \cdot 10^4$$

$$\text{Xylitol: } k_\infty = 1,4014 \cdot 10^{22} \quad E_A = 6,5695 \cdot 10^4$$

TABLE 3 | Modeling results of all three approaches.

Index	1st approach	
	$k\infty$ [1/min] (Ragauskas and Huang, 2013)	EA [J/(mol·K)]
Xylose	$1.4277 \cdot 1,019$	$8.0858 \cdot 10^4$
Xylitol	$1.4014 \cdot 1,022$	$6.5695 \cdot 10^4$

	2nd approach			3rd approach	
	$k\infty$ [1/min]	EA [J/(mol·K)]		k_∞ [1/min]	E_A [J/(mol·K)]
1	$1.0385 \cdot 10^6$	$3.7624 \cdot 10^4$		$8.7489 \cdot 10^5$	$5.9741 \cdot 10^4$
2	8.9181	$5.9280 \cdot 10^4$		$4.6303 \cdot 10^2$	$4.3998 \cdot 10^4$
3	82.0541	$1.4526 \cdot 10^4$		$2.1248 \cdot 10^2$	$2.6756 \cdot 10^4$
4	$1.4277 \cdot 10^{19}$	$8.0858 \cdot 10^4$		$4.0895 \cdot 10^{19}$	$8.7653 \cdot 10^4$
5	$1.3862 \cdot 10^5$	$2.3632 \cdot 10^6$		0	1
6	$3.2223 \cdot 10^3$	$2.4760 \cdot 10^4$		1	1
7	$1.0480 \cdot 10^4$	$1.4960 \cdot 10^4$		$8.7489 \cdot 10^3$	$5.9259 \cdot 10^3$
8	$1.4014 \cdot 10^{22}$	$6.5695 \cdot 10^4$		$1.1033 \cdot 10^{22}$	$6.3132 \cdot 10^4$
9	$8.1253 \cdot 10^3$	$2.5667 \cdot 10^5$		$1.0251 \cdot 10^4$	$1.7651 \cdot 10^5$
10	6.0908	$5.3484 \cdot 10^3$		$8.3279 \cdot 10^2$	$3.8088 \cdot 10^3$

The mean error $R = 4.25\%$ was even slightly higher with this much more detailed model, thus we decided that more literature research and rigorous model modification was needed.

Third Approach: Modified Complex Model

The ongoing literature review during the kinetic studies revealed two additional factors that had not been considered in our complex model. Therefore, we needed to develop a third approach which included the following two concepts into our own modified model. One aspect regards the complex nature of hemicelluloses, specifically xylan molecules and introduces the effect of two parallel hydrolysis reactions with significantly different reaction rates (Salmi et al., 2014b). The other aspect focuses on the overall possible product yield, because depending on the type of hemicellulose the xylose content varies to a large extent (Polizeli et al., 2005; Ragauskas and Huang, 2013). This fact leads to very different maximum yields, which needs to be attributed into the model, otherwise distorting the carbon balance for xylose and xylitol, respectively, by significantly large relative errors (up to ca. 20%). A realistic common xylose yield from hydrolysis of different xylan species was mentioned to be about 85%, according to (Mäki-Arvela et al., 2011). Similar values for polyols were mentioned in a different study (Köchermann et al., 2018), thus leading to a mean possible xylitol yield of 85% as well.

In addition to the literature-based modifications, we also relied on the modeling results from the first two approaches for further simplification and optimization. For example, the thermal decomposition of xylose (denoted as parameter constant "k_5") is negligible in comparison to the fast hydrogenation of the relatively low amounts of post-hydrolysis released xylose molecules. Another parameter constant, which was identified to allow adjustment, was the factor "k_6" that describes the hydrogen adsorption on the catalyst surface. Justification for the adjustment came from two observations. First, the pre-experiment catalyst activation with pressurized hydrogen at elevated results in a catalyst surface whereon all precious metal sites have been reduced by hydrogen and are therefore highly active, and additionally the catalyst surface should be practically close to hydrogen-saturation (with proper catalyst storage). Second, the amount of dissolved hydrogen within the aqueous solution, in addition to the tiny hydrogen bubbles from the gas entrainment stirring, provides excess hydrogen compared to the relatively low xylose concentrations and the linked hydrogen requirement due to the catalytic hydrogenation reactions. Thus, one can safely assume that the overall hydrogen adsorption onto the catalyst surface ("k_6") is much faster, than the xylitol desorption after successful xylose hydrogenation.

During the development of the third approach, the presented model modifications have been tested in several combinations of each other. **Table 2** shows the relative errors of each model variation.

TABLE 4 | Values for kinetic model parameters from related literature for comparison.

Subject	E_A [J/mol]	k_∞	References
Hydrolysis of arabinogalactan	$1.26 \cdot 10^5 – 1.35 \cdot 10^5$	$0.0147 – 0.142$	(Kusema et al., 2010)
Substitution of cellulose	$1.27 \cdot 10^5 – 1.40 \cdot 10^5$	$0.238 – 0.326$ L/(mol·min)	(Salmi et al., 2011)
Hydrogenation of arabinose and galactose	$5.68 \cdot 10 – 8.36 \cdot 10$	$11.5 – 43.8$ 1/s	(Sifontes Herrera et al., 2011)
	$5.64 \cdot 10 – 6.89 \cdot 10$	$712 – 4,660$ 1/s	(Sifontes Herrera et al., 2012)
Hydrolysis of hemicelluloses	n.a.	$0.23 \cdot 10^{-3} – 0.34 \cdot 10^{-3}$ L/(mol·min)	(Salmi et al., 2014b)
Hydrolysis of xylan	$1.43 \cdot 10^5$	$1.42 \cdot 10^{17}$ 1/(min·(wt%/v)^2)	(Kanchanalai et al., 2016)
Hydrolysis of rice straw	$1.12 \cdot 10^4 – 1.56 \cdot 10^4$	n.a	(Mukherjee et al., 2017)
Hydrolysis of birchwood	$4.96 \cdot 10^4 – 5.17 \cdot 10^4$	$4.2610^3 – 6.6310^9$ 1/min	(Nakasu et al., 2017)

Finally, the combination of parameter adjustments for k_5 and k_6 in addition to including realistic maximum possible yields for xylose and xylitol delivered improved modeling results with a mean error R of 3.96%. The respective graphical plots for this selected model modification are shown in **Figure 5**.

The model fit for xylose curves is much better than with the first and second approach, while the model fit for xylitol is slightly off during the plateau phase when the reaction nears the maximum xylitol yield. This is attributed to the necessary Matlab calculations which needed to be given end limits. However, with regards to the research aim of process intensification with higher space-time-yields, the rate-limiting step of xylose release from the bulk xylan should be considered more important than the (much faster) xylose hydrogenation to xylitol. In **Table 3** we present all modeling results of the best calculations/model variants of all three different approaches.

The third approach delivered model results which were increasingly more accurate with higher temperatures, regardless of the end yield, but with focus on the reaction rate (for literature comparison see **Table 4**). As industrial applications will certainly try to realize a process in a continuous matter, the thermal decomposition can be handled safely by limiting the residence time in the reactor, for example. Therefore, we think that our last approach is a workable kinetic model for the one-pot hydrolytic hydrogenation of xylan to xylitol and is ready for validation tests or further optimization in (semi-) industrial contexts.

CONCLUSION AND OUTLOOK

We investigated the one-pot hydrolytic hydrogenation of xylan to xylitol, an economically attractive and versatile sugar alcohol product. The one-pot process can be an efficient alternative to the conventional two-step process of hydrolysis followed by hydrogenation, conducted in separate reactors.

The investigations on the theoretical background for reaction kinetics of xylan conversion via intermediate xylose production and subsequent hydrogenation to xylitol showed that often a standard empirical (second order kinetics) model can deliver satisfactory results. In our case, this relatively simple model had a mean error R of 4.03%. We then developed a more complex model with respect to most of the detailed reaction steps from the overall reaction mechanism. This second approach was a slight setback in terms of its $R = 4.25\%$. Thus, a vigorous refinement of the complex model was realized during our third approach with a good model fit as result ($R = 3.96\%$). We therefore recommend the refined complex model for future biorefinery process design.

Further modeling work should try to exclude the experimental values from the beginning of each experiment (0 . . . 20–30 min) where diverging heat-up rates of the reactor system might have caused different delayed reaction initiations. This might have contributed to remaining numerical shortcomings of the model.

DATA AVAILABILITY STATEMENT

The raw data supporting the conclusions of this article will be made available by the authors, without undue reservation.

AUTHOR CONTRIBUTIONS

GH wrote the manuscript, managed the research project and co-developed the models, PK conducted calculations via matlab and modifications to the initial model, TR developed the initial model, conducted experiments and analysis, MMA did literature research, realized experimental work and improved analysis

ACKNOWLEDGMENTS

REFERENCES

Anwar, Z., Gulfraz, M., and Irshad, M. (2014). Agro-industrial lignocellulosic biomass a key to unlock the future bio-energy: a brief review. *J. Radiat. Res. Appl. Sci.* 7, 163–173. doi:10.1016/j.jrras.2014.02.003

Ayubi, M. M., Werner, A., Steudler, S., Haase, S., Lange, R., Walther, T., et al. (2020). Enhanced xylan conversion to xylitol in a bio- and chemocatalytic one-pot process. *Catal. Today* 12, 33–37. doi:10.1016/j.cattod.2020.06.009

Barbaro, P., Liguori, F., and Moreno-Marrodan, C. (2016). Selective direct conversion of C5 and C6 sugars to high added-value chemicals by a bifunctional, single catalytic body. *Green Chem.* 18, 2935–2940. doi:10.1039/C6GC00128A

Bigand, V., Pinel, C., Da Silva Perez, D., Rataboul, F., Huber, P., and Petit-Conil, M. (2011). Cationisation of galactomannan and xylan hemicelluloses. *Carbohydr. Polym.* 85, 138–148. doi:10.1016/j.carbpol.2011.02.005

Chheda, J. N., Huber, G. W., and Dumesic, J. A. (2007). Liquid-phase catalytic processing of biomass-derived oxygenated hydrocarbons to fuels and chemicals. *Angew. Chem. Int. Ed.* 46, 7164–7183. doi:10.1002/anie.200604274

Delgado Arcaño, Y., Valmaña García, O. D., Mandelli, D., Carvalho, W. A., and Magalhães Pontes, L. A. (2020). Xylitol: A review on the progress and challenges of its production by chemical route. *Catal. Today* 344, 2–14. doi:10.1016/j.cattod.2018.07.060

Dietrich, K., Hernandez-Mejia, C., Verschuren, P., Rothenberg, G., and Shiju, N. R. (2017). One-pot selective conversion of hemicellulose to xylitol. *Org. Process Res. Dev.* 21, 165–170. doi:10.1021/acs.oprd.6b00169

Fagerstedt, K., Mellerowicz, E., Gorshkova, T., Ruel, K., and Joseleau, J.-P. (2014). "Cell wall polymers in reaction wood," in *The biology of reaction wood*. Editors B. Gardiner, J. Barnett, P. Saranpää, and J. Gril (Berlin: Springer), 37–106. doi:10.1007/978-3-642-10814-3

Gellerstedt, G., and Henriksson, G. (2009). *Hemicelluloses, pectins, pulp and paper chemistry and technology 1, wood chemistry and wood biotechnology*. Berlin: Walter De Gruyter, 101–120. doi:10.1515/9783110213409

González, G., López-Santín, J., Caminal, G., and Solà, C. (1986). Dilute acid hydrolysis of wheat straw hemicellulose at moderate temperature: a simplified kinetic model. *Biotechnol. Bioeng.* 28, 288–293. doi:10.1002/bit.260280219

Hernandez-Mejia, C., Gnanakumar, E. S., Olivos-Suarez, A., Gascon, J., Greer, H. F., Zhou, W., et al. (2016). Ru/TiO2-catalysed hydrogenation of xylose: the role of the crystal structure of the support. *Catal. Sci. Technol.* 6, 577–582. doi:10.1039/C5CY01005E

Hilpmann, G., Becher, N., Pahner, F. A., Kusema, B., Mäki-Arvela, P., Lange, R., et al. (2016). Acid hydrolysis of xylan, *Catal. Today* 259 (Part 2), 376–380. doi:10.1007/s10562-018-2598-7

Hilpmann, G. (2017). *Process intensification via catalytic one-pot conversion of hemicelluloses to sugar alcohols (PhD thesis)*. Dresden: Fakultät maschinenwesen. Technische Universität.

Hilpmann, G., Steudler, S., Ayubi, M. M., Pospiech, A., Walther, T., Bley, T., et al. (2019). Combining chemical and biological catalysis for the conversion of hemicelluloses: hydrolytic hydrogenation of xylan to xylitol. *Catal. Lett.* 149, 69–76. doi:10.1007/s10562-018-2598-7

Jacobsen, S., and Wyman, C. (2000). "Cellulose and hemicellulose hydrolysis models for application to current and novel pretreatment processes," in *Twenty-first symposium on biotechnology for fuels and chemicals*. Editors M. Finkelstein, and B. Davison (Totowa: Humana Press), 81–96. doi:10.1385/ABAB:84-86:1-9:81

Ji, X.-J., Huang, H., Nie, Z.-K., Qu, L., Xu, Q., and Tsao, G. (2012). "*Fuels and chemicals from hemicellulose sugars*", in F.-W. Bai, C.-G. Liu, H. Huang, and G. T. Tsao, (Eds.), *Biotechnology in China III: biofuels and bioenergy*, (Berlin: Springer), pp. 199–224. doi:10.1007/10_2011_124

Kamm, B., and Kamm, M. (2004). Principles of biorefineries. *Appl. Microbiol. Biotechnol.* 64, 137–145. doi:10.1007/s00253-003-1537-7

Kanchanalai, P., Temani, G., Kawajiri, Y., and Realff, M. J. (2016). Reaction kinetics of concentrated-acid hydrolysis for cellulose and hemicellulose and effect of crystallinity *BioResources* 11, 18. doi:10.15376/biores.11.1.1672-1689

Köchermann, J., Mühlenberg, J., and Klemm, M. (2018). Kinetics of hydrothermal furfural production from organosolv hemicellulose and d-xylose. *Ind. Eng. Chem. Res.* 57, 14417–14427. doi:10.1021/acs.iecr.8b03402

Kusema, B. T., Xu, C., Mäki-Arvela, P., Willför, S., Holmbom, B., Salmi, T., et al. (2010). Kinetics of acid hydrolysis of Arabinogalactans. *Int. J. Chem. React. Eng.* 8, 1. doi:10.2202/1542-6580.2118

Li, X., Guo, T., Xia, Q., Liu, X., and Wang, Y. (2018). One-pot catalytic transformation of lignocellulosic biomass into alkylcyclohexanes and polyols. *ACS Sustain. Chem. Eng.* 6, 4390–4399. doi:10.1155/2018/4723573

Li, X., Yang, J., Xu, R., Lu, L., Kong, F., Liang, M., et al. (2019). Kinetic study of furfural production from Eucalyptus sawdust using H-SAPO-34 as solid Brønsted acid and Lewis acid catalysts in biomass-derived solvents. *Ind. Crop. Prod.* 135, 196–205. doi:10.1016/j.indcrop.2019.04.047

Liu, C.-J., Zhu, N.-N., Ma, J.-G., and Cheng, P. (2019). Toward green production of chewing gum and diet: complete hydrogenation of xylose to xylitol over ruthenium composite catalysts under mild conditions. *Research* 2019, 5178573. doi:10.34133/2019/5178573

Liu, X., Lu, M., Ai, N., Yu, F., and Ji, J. (2012). Kinetic model analysis of dilute sulfuric acid-catalyzed hemicellulose hydrolysis in sweet sorghum bagasse for xylose production. *Ind. Crop. Prod.* 38, 81–86. doi:10.1016/j.indcrop.2012.01.013

Lu, Y., and Mosier, N. S. (2008). Kinetic modeling analysis of maleic acid-catalyzed hemicellulose hydrolysis in corn stover. *Biotechnol. Bioeng.* 101, 1170–1181. doi:10.1002/bit.22008

Mäki-Arvela, P., Salmi, T., Holmbom, B., Willför, S., and Murzin, D. Y. (2011). Synthesis of sugars by hydrolysis of hemicelluloses-A review. *Chem. Rev.* 111, 5638–5666. doi:10.1021/cr2000042

Mukherjee, A., Mandal, T., Ganguly, A., Ghosh, P. S., and Chatterjee, P. K. (2017). Investigations on the kinetics of acid catalyzed hemicellulose hydrolysis derived from waste rice straw for the production of bio-ethanol. *Indian J. Sci. Technol.* 10, 1–8. doi:10.1155/2017/4876969

Nakasu, P. Y. S., Chagas, M. F., Costa, A. C., and Rabelo, S. C. (2017). Kinetic study of the acid post-hydrolysis of xylooligosaccharides from hydrothermal pretreatment. *BioEnergy Res.* 10, 1045–1056. doi:10.1007/s12155-017-9864-1

Polizeli, M. L. T. M., Rizzatti, A. C. S., Monti, R., Terenzi, H. F., Jorge, J. A., and Amorim, D. S. (2005). Xylanases from fungi: properties and industrial applications. *Appl. Microbiol. Biotechnol.* 67, 577–591. doi:10.1007/s00253-005-1904-7

Ragauskas, A. J., and Huang, F. (2013). "Chemical pretreatment techniques for biofuels and biorefineries from softwood," in *Pretreatment techniques for biofuels and biorefineries*. Editor Z. Fang (Berlin: Springer), 151–179. doi:10.1007/978-3-642-32735-3

Renard, D., Lavenant-Gourgeon, L., Lapp, A., Nigen, M., and Sanchez, C. (2014). Enzymatic hydrolysis studies of arabinogalactan-protein structure from Acacia gum: the self-similarity hypothesis of assembly from a common building block. *Carbohydr. Polym.* 112, 648–661. doi:10.1016/j.carbpol.2014.06.041

Ribeiro, L. S., Delgado, J. J., de Melo Órfão, J. J., and Ribeiro Pereira, M. F. (2016). A one-pot method for the enhanced production of xylitol directly from hemicellulose (corncob xylan). *RSC Adv.* 6, 95320–95327. doi:10.1039/C6RA19666G

Ribeiro, L. S., Órfão, J. J. M., and Pereira, M. F. R. (2017). Screening of catalysts and reaction conditions for the direct conversion of corncob xylan to xylitol. *Green Process. Synth.* 6, 265. doi:10.1515/gps-2016-0174

Saleh, M., Cuevas, M., García, J. F., and Sánchez, S. (2014). Valorization of olive stones for xylitol and ethanol production from dilute acid pretreatment via enzymatic hydrolysis and fermentation by *Pachysolen tannophilus*. *Biochem. Eng. J.* 90, 286–293. doi:10.1016/j.bej.2014.06.023

Salmi, T., Damlin, P., Mikkola, J.-P., and Kangas, M. (2011). Modelling and experimental verification of cellulose substitution kinetics. *Chem. Eng. Sci.* 66, 171–182. doi:10.1016/j.ces.2010.10.013

Salmi, T., Murzin, D., Wärnå, J., Mäki-Arvela, P., Kusema, B., Holmbom, B., et al. (2014a). Hemicellulose hydrolysis in the presence of heterogeneous catalysts. *Top. Catal.* 29 1–6. doi:10.1007/s11244-014-0320-6

Salmi, T., Murzin, D. Y., Mäki-Arvela, P., Kusema, B., Holmbom, B., Willför, S., et al. (2014b). Kinetic modeling of hemicellulose hydrolysis in the presence of homogeneous and heterogeneous catalysts. *AIChE J.* 60, 1066–1077. doi:10.1002/aic.14311

Sedlmeyer, F. B. (2011). Xylan as by-product of biorefineries: characteristics and potential use for food applications. *Food Hydrocolloids* 25, 1891–1898. doi:10.1016/j.foodhyd.2011.04.005

Sharkov, V. I. (1963). Production of polyhydric alcohols from wood polysaccharides. *Angew Chem. Int. Ed. Engl.* 2, 405–409. doi:10.1002/anie.196304051

Sifontes Herrera, V. A., Oladele, O., Kordás, K., Eränen, K., Mikkola, J.-P., Murzin, D. Y., et al. (2011). Sugar hydrogenation over a Ru/C catalyst. *J. Chem. Technol. Biotechnol.* 86, 658–668. doi:10.1002/jctb.2565

Sifontes Herrera, V. A., Saleem, F., Kusema, B., Eränen, K., and Salmi, T. (2012). Hydrogenation of l-arabinose and d-galactose mixtures over a heterogeneous Ru/C catalyst. *Top. Catal.* 55, 550–555. doi:10.1007/s11244-012-9833-z

Sun, Y., and Cheng, J. (2002). Hydrolysis of lignocellulosic materials for ethanol production: a review. *Bioresour. Technol.* 83, 1–11. doi:10.1016/s0960-8524(01)00212-7

Teleman, A., Tenkanen, M., Jacobs, A., and Dahlman, O. (2002). Characterization of O-acetyl-(4-O-methylglucurono)xylan isolated from birch and beech. *Carbohydr. Res.* 337, 373–377. doi:10.1016/s0008-6215(01)00327-5

Testova, L., Chong, S.-L., Tenkanen, M., and Sixta, H. (2011). *Autohydrolysis of birch wood*. Vienna: Holzforschung, 535. doi:10.1515/hf.2011.073

Vandenbossche, V., Brault, J., Vilarem, G., Hernández-Meléndez, O., Vivaldo-Lima, E., Hernández-Luna, M., et al. (2014). A new lignocellulosic biomass deconstruction process combining thermo-mechano chemical action and bio-catalytic enzymatic hydrolysis in a twin-screw extruder. *Ind. Crop. Prod.* 55, 258–266. doi:10.1016/j.indcrop.2014.02.022

Vasyunina, N. A., Balandin, A. A., Chepigo, S. V., and Barysheva, G. S. (1960). Catalytic hydrogenation of wood and other vegetable materials. *Bull. Acad. Sci.* 9, 1419.

Westbye, P., Köhnke, T., and Gatenholm, P. (2008). *Fractionation and characterization of xylan rich extracts from birch*. Vienna: Holzforschung, 31. doi:10.1515/HF.2008.005

Wirsching, S. G. (2014). *Bioökonomie in deutschland*. Bonn, Berlin: BMBF & BMEL.

Yamaguchi, A., Mimura, N., Shirai, M., and Sato, O. (2019). Cascade utilization of biomass: strategy for conversion of cellulose, hemicellulose, and lignin into useful chemicals. *ACS Sustain. Chem. Eng.* 7, 10445–10451. doi:10.1021/acssuschemeng.9b00786

Zhao, X., Morikawa, Y., Qi, F., Zeng, J., and Liu, D. (2014). A novel kinetic model for polysaccharide dissolution during atmospheric acetic acid pretreatment of sugarcane bagasse. *Bioresour. Technol.* 151, 128–136. doi:10.1016/j.biortech.2013.10.036

Zhu, T., Li, P., Wang, X., Yang, W., Chang, H., and Ma, S. (2014). Optimization of formic acid hydrolysis of corn cob in xylose production. *Kor. J. Chem. Eng.* 31, 1624–1631. doi:10.1007/s11814-014-0073-8